ChemPubSoc Europe

DOI: 10.1002/batt.201800050

BATTERIES & SUPERCAPS Communications

Extent of Pseudocapacitance in High-Surface Area Vanadium Nitrides

Abdoulaye Djire,*[a] Olabode Ajenifujah,[a] and Levi T. Thompson*[a, b]

Early transition-metal nitrides, especially vanadium nitride (VN), have shown promise for use in high energy density supercapacitors due to their high electronic conductivity, areal specific capacitance, and ability to be synthesized in high surface area form. Their further development would benefit from an understanding of their pseudocapacitive charge storage mechanism. In this paper, the extent of pseudocapacitance exhibited by vanadium nitride in aqueous electrolytes was investigated using cyclic voltammetry and electrochemical impedance spectroscopy. The pseudocapacitance contribution to the total capacitance in the nitride material was much higher than the double-layer capacitance and ranged from 85% in basic electrolyte to 87% in acidic electrolyte. The mole of electrons transferred per VN material during pseudocapacitive charge storage was also evaluated. This pseudocapacitive charge-storage is the key component in the full utilization of the properties of early-transition metal nitrides for high-energy density supercapacitors.

1. Introduction

Recently, early transition-metal nitrides have been reported as potential electrode materials for supercapacitor applications. The nitride materials can be produced with desirable properties including; highly accessible surface area, high electric conductivity and at low cost.[1–10] They possess high capacitance, good capacitance retention during cycling and exhibit wide voltage windows.[11–16] For example, the capacitance for vanadium nitride (VN) has been reported to be as high as 1340 Fg^{-1} in aqueous alkaline electrolyte.[12] The origin of this high capacitance was attributed to a combination of electric double-layer formation and faradaic redox reactions occurring on the nitride or oxynitride (VN_xO_y) surface.[12] However, the contribution of each mechanism has not been quantified. This is difficult to quantitatively determine; especially on bulk powder electrodes due to complex fractal geometry of the nanometer-sized, agglomerates, and the heterogeneous crystallographic sites present.[12] Despite efforts to date, the extent of pseudocapacitance in early transition-metal nitrides remains unknown. Here we report the pseudocapacitance contribution to the total capacitance for vanadium nitride in aqueous media using cyclic voltammetry and electrochemical impedance spectroscopy analyses. The pseudocapacitive contribution ranges from 85% in basic electrolyte to 87% in aqueous acidic electrolyte.

[a] Dr. A. Djire, O. Ajenifujah, Prof. L. T. Thompson
Department of Chemical Engineering
University of Michigan
Ann Arbor, MI 48109-2136, USA
E-mail: adjire@umich.edu
ltt@umich.edu
[b] Prof. L. T. Thompson
Department of Mechanical Engineering and
Hydrogen Energy Technology Laboratory
University of Michigan
Ann Arbor, MI 48109–2136, USA

Experimental

Material Synthesis

High-surface-area vanadium nitride was prepared from its oxide precursor, V_2O_5 (Alfa Aesar) by temperature-programmed reaction (TPR) synthesis with NH_3 (Cryogenic Gases).[13–16] The oxide precursor was supported on a quartz-wool plug in a quartz tube reactor. After synthesis, the material was quenched to room temperature and then passivated using a flowing mixture of 1% O_2/He (Cryogenic Gases) to form an oxygen-rich protective layer that prevents oxidation of the bulk material when exposed to air.

Physical Characterization

The surface areas and pore size distribution of vanadium nitride material was determined by N_2 physisorption using a Micrometrics ASAP 2010 analyzer with the Brunauer–Emmett–Teller (BET) method and Barrett-Joiner-Helenda (BJH) method, respectively. Prior to analysis, the material was degassed in vacuum at 350 °C for 24 hours. The material was then characterized by X-ray diffraction (XRD) using a Rigaku Miniflex Diffractometer with Cu Kα ($\lambda = 0.15404$ nm) source. The XRD was carried out at a scan rate of 5.0° min^{-1} with a step size of 0.1° over a 2θ range of 10° to 90°. The JADE 10.0 software was used for peak identification.

Electrochemical Characterization

The electrochemical characterization was carried out using cyclic voltammetry (CV) and electrochemical impedance spectroscopy (EIS) in a three-electrode electrochemical cell (ECC-Aqu, EL-Cell GmbH, Germany) with 0.1 mol dm^{-3} H_2SO_4 and 0.1 mol dm^{-3} KOH electrolytes. The cell was assembled with an 18 mm diameter glass fiber separator of thickness 1.55 mm. An 18 mm diameter counter electrode (Kynol activated carbon

fabric ACC-507-15, sp. S. A. 1500 $m^2 g^{-1}$, thickness 0.54 mm) was used. The working electrode was prepared by mixing the synthesized material (92 wt.%), carbon black (5 wt.%, Super PLi (TIMCAL) and polyvinylidene fluoride (3 wt.%, Kynar) in N-methylpyrrolidione solvent (Alfa Aesar). The resulting slurry was spread onto a Ti foil and then dried in vacuum at 80 °C for 8 hours. The mass of the active material was determined by subtracting the mass of the Ti substrate from the mass of the coated electrode (Ti + active material). The active material coated on the substrate was 3 mg. The working electrode diameter was 16 mm, to ensure better current flow between counter and working electrodes. A Pt wire (1 mm diameter) was used as the quasi-reference electrode. Pt wire electrode has been shown to be electrochemically stable in aqueous electrolytes, and can be used as a reference electrode under appropriate conditions.[16] The counter electrode and separator were soaked in electrolyte overnight, to ensure better wettability; and deaereated with nitrogen for at least 30 min before assembling the cell. The measurements were performed using an Autolab PGSTAT302N potentiostat. Prior to characterizing the working electrode, blank measurements were taken on the carbon and PVDF binder electrode in both acidic and basic electrolytes.

CV was used to determine the total capacitance in aqueous electrolytes. EIS analysis was used to measure the pseudocapacitance and double-layer capacitance. EIS has been recognized as one of the principal methods for examining the fundamental behavior of electrode materials. EIS measurements were performed at selected potentials within the stable potential window. A low amplitude modulation of 10 mV and a wide frequency range from 1 mHz to 100 kHz were used.

2. Results and Discussion

2.1 Performance Evaluation

The XRD patterns shown in Figure 1a confirmed that the material was phase-pure VN. Pore size distributions indicated the presence of micropores (< 2 nm) and some mesoporosity (2-50 nm) (see Figure 1b). The average pore sizes determined using the BJH method was 19 ± 2 nm. The SEM micrograph shown in Figure 1c indicated that the synthesized VN material is highly porous, consistent with the adsorption measurements. Table 1 summarizes the physical and electrochemical properties of VN in aqueous electrolytes. The surface area obtained for the synthesized material is similar to those reported in the literature.[11–17] The areal specific capacitances, normalized by the surface area (obtained from N_2 physisorption) were estimated by integrating the area under the voltammograms and dividing by the nitride mass loading.[13] The voltage window (shown in Table 1) is taken as the width of the voltammogram. The areal specific capacitances measured in both basic and acidic electrolytes are much higher than the expected double-layer capacitance for porous materials (typically, 20–50 μF cm^{-2}).[14] This indicates the presence of pseudocapacitive charge-storage mechanism in VN in aqueous electrolytes.[14]

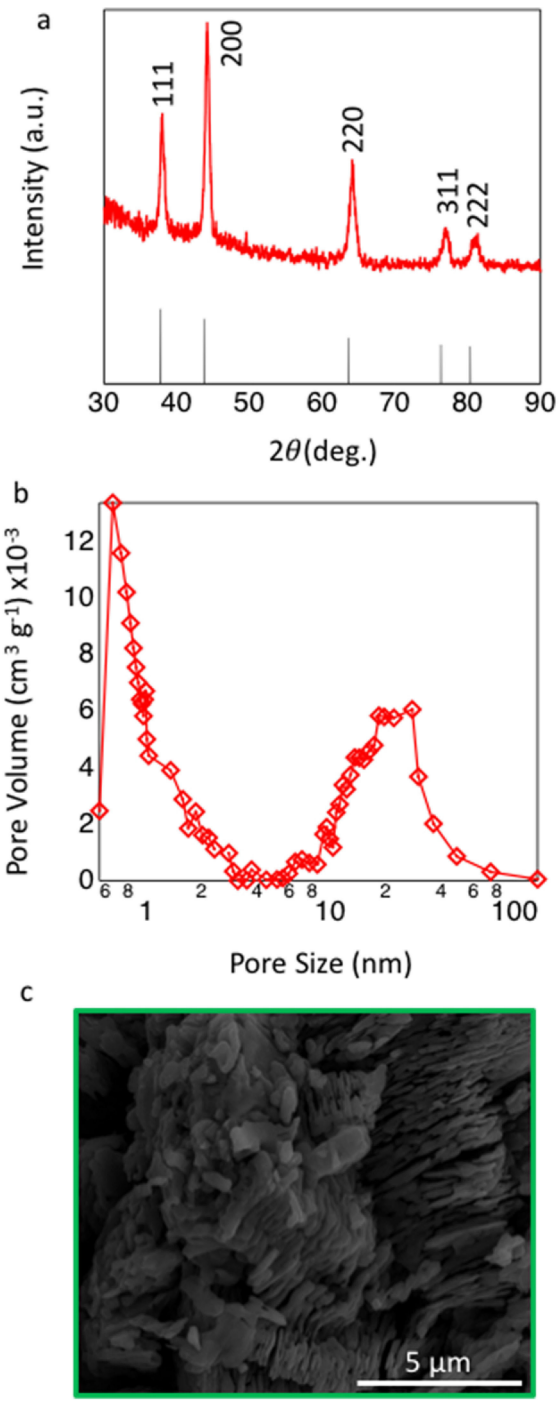

Figure 1. a) X-ray diffraction patterns (PDF # 01-074-8389), b) pore size distribution and c) scanning electron microscopy image for VN.

2.2 Extent of Pseudocapacitance

EIS was used to quantitatively determine the extent of pseudocapacitance in VN material in aqueous electrolytes. Figures 2 (a and b) shows the phase angle as function of

Table 1. Surface area, voltage window, normalized capacitance, extent of pseudocapacitance, and mole of electron transferred for vanadium nitride in aqueous electrolytes.

Material	Surface area [$m^2 g^{-1}$]	Voltage window [V]	Areal specific capacitance [$\mu F\,cm^{-2}$]	Extent of pseudo-capacitance [%]	Mole of e^- per mole of material loading
VN	38	1.1 (H_2SO_4)	350	87	0.11
		1.1 (KOH)	610	85	0.13

frequency (Bode plot) for VN in aqueous electrolytes at selected potentials within the stable potential window. The total capacitive behavior of the system is obtained at low frequency where the phase angle approaches a maximum value.[18,19] At that frequency, the derivative of the phase angle with respect to frequency goes to zero as shown in Equation (1) below:

$$\frac{d\emptyset}{df} = 0, \ when \ f = \ f_{max} \tag{1}$$

where Φ and f_{max} are the phase angle and maximum frequency, respectively. At a potential where only double-layer or electrostatic charge forms, the derivative of the phase angle goes to zero faster (at a higher frequency) than at a potential where pseudocapacitive storage also occurs as shown in Figures 2 (c and d). This agrees with the fact that the two charge-storage mechanisms have different time constants. The double layer time constant is faster than the pseudocapacitive time constant.

The capacitance at each selected potential was calculated using Equation (2):[20,21]

$$C = \frac{-1}{2\pi f_{max} Z''_{max}} \tag{2}$$

where Z''_{max} is the imaginary impedance at the maximum frequency f_{max}. Table 2 lists the Z''_{max}, f_{max} and capacitance values for VN material in aqueous electrolytes. A plot of capacitance versus potential allows distinction between double-layer charge and pseudocapacitive charge, which generally varies with applied voltage. As mentioned earlier, the total capacitive behavior of the system was obtained at a maximum phase angle, near −90°, where the system behaves like an ideal supercapacitor.[18,19]

Figures 3 (a and b) show the areal specific capacitance for VN as a function of scan rate in aqueous electrolytes. The capacitances at low scan rates are significantly higher than those expected for double layer capacitance (typically, ~50 $\mu F\,cm^{-2}$ for porous materials) and decreased logarithmically with increasing scan rate, consistent with a pseudocapacitive charge storage mechanism.[14,17] Figures 3 (c and d) show the capacitances obtained from EIS (red markers) plotted on top of the cyclic voltammograms for VN material at selected

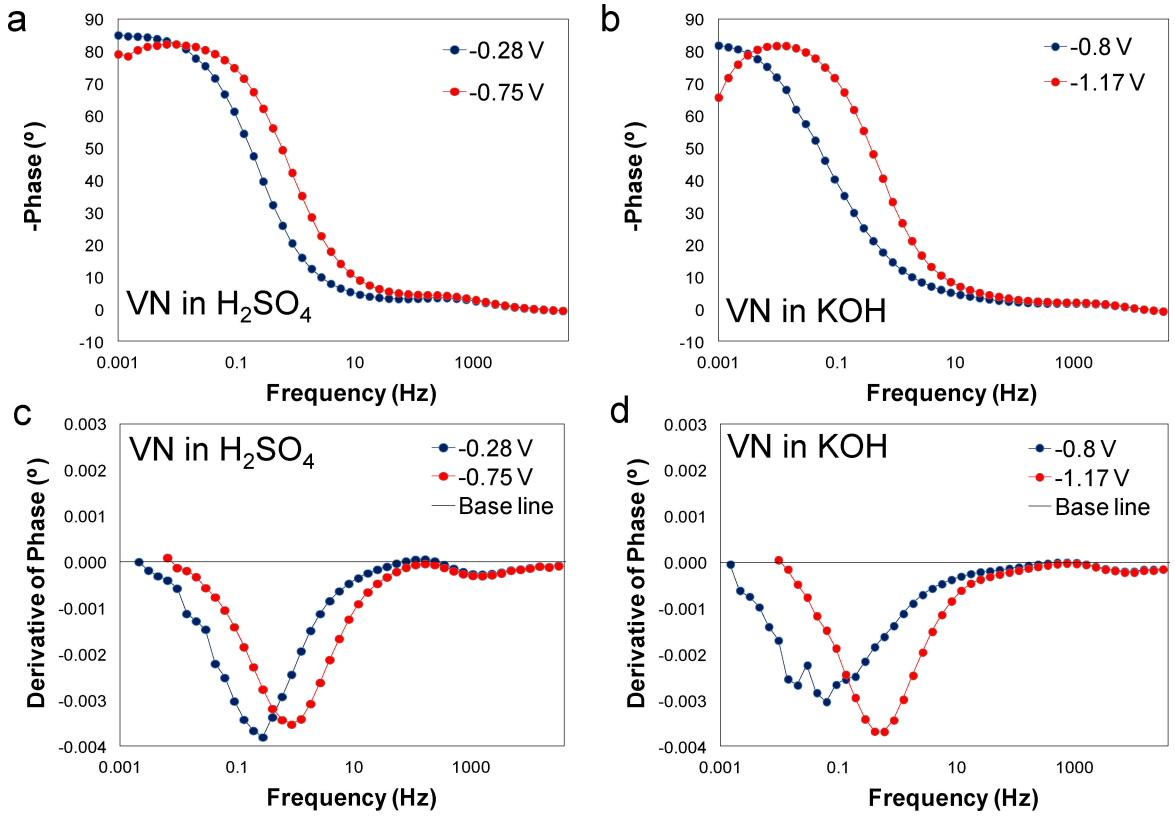

Figure 2. a), b) Plot of Bode phase angle and c), d) the derivative of Bode phase angle as function of frequency for VN in 0.1 M H_2SO_4 and 0.1 M KOH at selected potentials within the stable potential window.

Table 2. Capacitance, Z''_{max} and f_{max} values for vanadium nitride in aqueous electrolytes at selected potentials within the stable voltage window, all data obtained from EIS.

VN (H_2SO_4) Potential [V]	Z''_{max}	f_{max}	Capacitance [F g^{-1}]	Specific capacitance [μF cm^{-2}]
−1.10	45.735	0.02947	41.00	102.49
−0.80	234.69	0.00954	24.68	61.70
−0.75	242.19	0.0095411	23.91	59.78
−0.65	154.31	0.013895	25.77	64.43
−0.45	212.48	0.0044984	57.81	144.52
−0.35	544.86	0.0014563	69.64	174.09
−0.28	679.12	0.001	81.36	203.41
VN (KOH) Potential [V]	**Z''_{max}**	**f_{max}**	**Capacitance [F g^{-1}]**	**Specific capacitance [μ cm^{-2}]**
−1.20	117.75	0.013895	33.77	84.43
−1.17	118.67	0.013895	33.51	83.77
−1.00	869.75	0.001	63.53	158.82
−0.85	308.33	0.001	179.21	448.02
−0.63	66.869	0.0065512	126.13	315.33
−0.40	647.2	0.001	85.38	213.44
−0.05	214.84	0.0044984	57.17	142.93

potentials within the stable voltage window. Interestingly, the capacitance goes to a minimum value in the double-layer region (which is typically the flat region on the CV) indicating absence of Faradaic redox reaction or pseudocapacitance. The double-layer capacitance in aqueous electrolytes is highlighted in red in Table 2. Note that the contribution to the total capacitance from the carbon support and PVDF binder was negligible. The capacitance increases at the potentials where redox reactions occurred, revealing the presence of pseudocapacitive charge storage.[12–16,22-26]

The extent of pseudocapacitance in VN material in aqueous electrolytes was determined by subtracting the double-layer capacitance from the total capacitance (listed on Table 1). The extent of the pseudocapacitive charge-storage contribution ranges from 85% in basic electrolyte to 87% in acidic electrolyte. This indicates that pseudocapacitance is the dominant charge-storage mechanism in nitrides. This high pseudocapacitance observed for the vanadium nitride is most likely due to its electroactive nature, which allows for multiple oxidation state changes during electrochemical cycling.[27–35] This explains why the areal specific capacitances (see Table 1) are much higher than that for activated carbons (11 μF cm^{-2}), the material in commercial supercapacitor devices.[29,30] The number of mole of

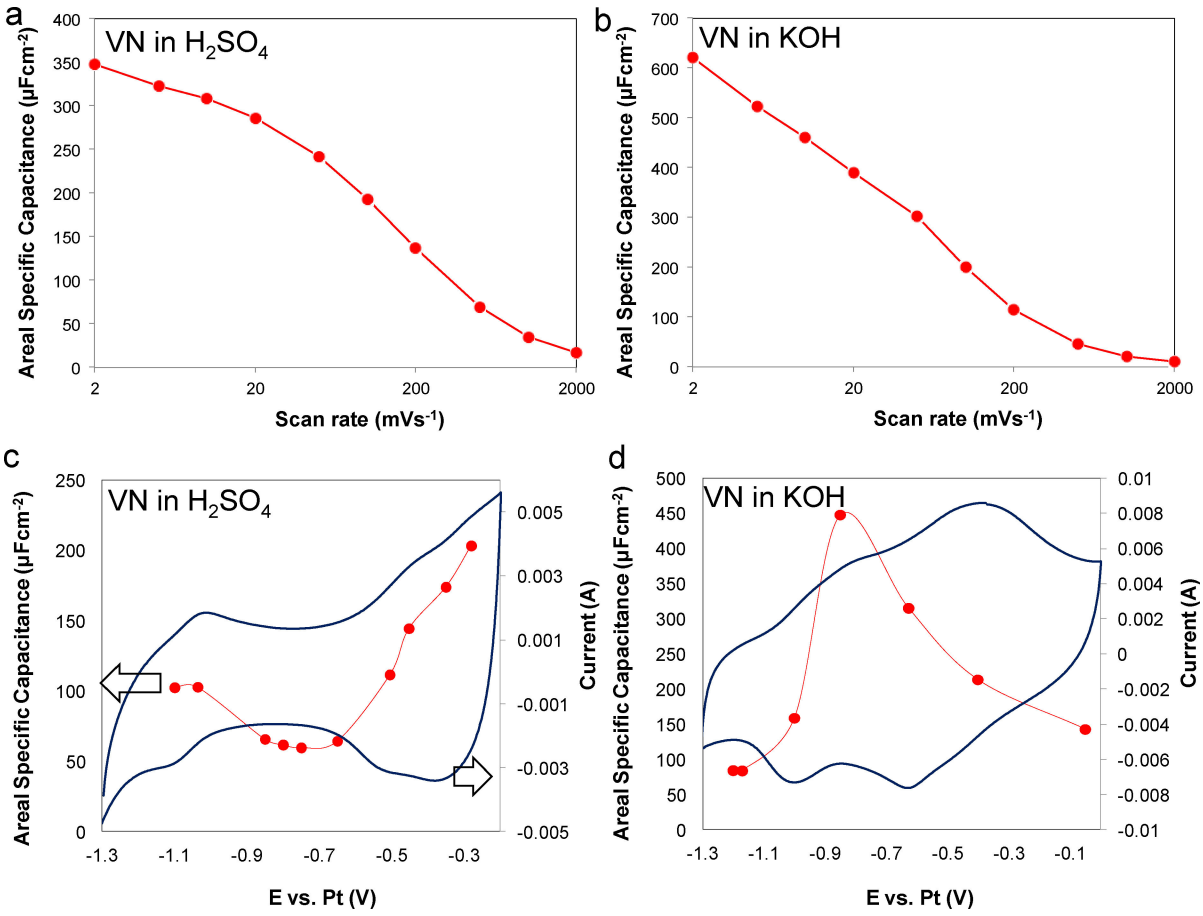

Figure 3. a), b) Plot of capacitance as function of scan rate and c), d) plot of capacitance (red dot circle) as function of potential and cyclic voltammogram of VN in 0.1 M H_2SO_4 and 0.1 M KOH; cyclic voltammogram measurements were performed using a scan rate of 10 mV/s and at room temperature. The scan shown is the 5th.

electron transferred during pseudocapacitive charge storage was determined by dividing the amount of pseudocapacitive charge by the Faradaic constant. As shown in Table 1, the mole of electrons transferred per mole of nitride (mass of coated material divided by the molecular weight) in both acidic and basic electrolytes was relatively low. Due to its electroactive nature, one would expect the ratio of mole of electron to mole of nitride material to be at least 1 or higher.[16] One plausible explanation to this discrepancy is the lack of full utilization of the nitride material during electrochemical cycling. Another explanation originates from the fact that pseudocapacitance involves more than one electrochemical process. The electrochemical processes that give rise to the pseudocapacitance include redox reaction, electrosorption, and intercalation.[13,17] The use of thin-film electrodes would be most desirable in order to better correlate the mole of electron to the mole of nitride material during electrochemical charge storage.

3. Conclusion

The extent of pseudocapacitance in vanadium nitride was successfully quantified using electrochemical impedance spectroscopy and cyclic voltammetry. The pseudocapacitive charge-storage mechanism was found to be the most dominant mechanism. The extent of the pseudocapacitive charge-storage contribution ranges from 85% in basic electrolyte to 87% in acidic electrolyte. To this date, there is no literature on the amount or contribution of pseudocapacitance in the charge-storage mechanism of vanadium nitride. For the first time, the extent of pseudocapacitive charge storage in nitrides is provided. This pseudocapacitive charge-storage is the key component in the full utilization of carbide and nitride-based supercapacitor materials for energy storage.

Acknowledgments

The authors acknowledge financial support from the Automotive Research Center, Army Tank Command and Army Research Office (W911NF-11-1-0465).

Conflict of Interest

The authors declare no conflict of interest.

Keywords: double-layer capacitance · energy storage · nitrides · pseudocapacitance · transition metals

Manuscript received: June 28, 2018
Version of record online: August 1, 2018

[1] R. B. Levy, M. Boudart, *Science* **1973**, *181*, 547–549.
[2] R. Kapoor, S. T. Oyama, *J. Solid State Chem.* **1992**, *99* 213–421.
[3] J. A. Schaidle, A. C. Lausche, L. T. Thompson, *J. Catal.* **2010**, 47, 235–272.
[4] J. G. Chen, *Chem. Rev.* **1996**, *96*, 4, 1477–1498.
[5] S. Ramanathan, St. T. Oyama, *J. Phys. Chem.* **1995**, *99*, 44, 16365–16372.
[6] J. S. Lee, M. Boudart, *Appl. Catal.* **1985**, *19*, 207–210.
[7] F. Shahzad, M. Alhabeb, C. B. Hatter, B. Anasori, S. M. Hong, C. M. Koo, Y. Gogotsi, *Science* **2016**, *6304*, 1137–1140.
[8] B. Anasori, M. R. Lukatskaya, Y. Gogotsi, *Nat. Rev. Mater.* **2017**, *2*, 16098.
[9] Y. Zhong, X. Xia, F. Shi, J. Zhan, J. Tu, H. J. Fan, *Adv. Sci.* **2016**, *3*, 1500286.
[10] M. R. Wixom, D. J. Tarnowski, J. M. Parker, J. Q. Lee, P. L. Chen, I. Song, L. T. Thompson, *Mat. Res. Soc. Symp. Proc.* **1998**, *496*, 643.
[11] A. Djire, J. B. Siegel, O. Ajenifujah, L. He, L. T. Thompson, *Nano Energy* **2018**, *51*, 122–127.
[12] D. W. Choi, G. E. Blomgren, P. N. Kumta, *Adv. Mater.* **2006**, *18*, 1178–1182.
[13] A. Djire, O. Ajenifujah, A. S. Sleigtholme, P. Rasmussen, L. T. Thompson, *J. Power Sources* **2015**, *47*, 159–166.
[14] B. E. Conway, W. G. Pell, *J. Solid State Electrochem.* **2003**, *7*, 637–644.
[15] P. Pande, P. Rasmussen, L. T. Thompson, *J. Power Sources* **2012**, *207*, 212–215.
[16] P. Pande, A. Deb, A. S. Sleightholme, A. Djire, P. Rasmussen, J. Penner-Hahn, L. T. Thompson, *J. Power Sources* **2015**, *289*, 154–159.
[17] T. C. Liu, W. G. Pell, B. E. Conway, *J. Electrochem. Soc.* **1998**, *6* 1882–1888.
[18] E. Frackowiak, F. Beguin, *Carbon* **2011**, 39, 937–950.
[19] A. Portet, G. Yushin, Y. Gogotsi, *Carbon* **2007**, *45*, 2511–2518.
[20] L. Andrzej, *Electrochemical Impedance Spectroscopy and its Application*, Kluwer Academic/Plenum Publisher, NY, **2014**.
[21] M. E. Orazem, *Electrochemical Impedance Spectroscopy*, Wiley Publisher, NY, **2008**.
[22] A. Djire, J. Y. Ishimwe, S. Choi, L. T. Thompson, *Electrochem. Commun.* **2017**, *77*, 19–23.
[23] O. Kartachova, A. M. Glushenkov, Y. Chen, H. Zhang, X. Dai, Y. Chen, *J. Power Sources* **2012**, 220, 298–305.
[24] O. Kartachova, A. M. Glushenkov, Y. Chen, H. Zhang, Y. Chen, *J. Mater. Chem. A* **2013**, *1*, 7889–7895.
[25] R. L. Porto, S. Bouhtiyya, J. F. Pierson, A. Morel, F. Caon, P. Boulet, T. Brousse, *Electrochim. Acta* **2014**, *141*, 203–211.
[26] M. R. Lukatskaya, S. -M Bak, X. -Q. Yang, M. W. Barsoum, Y. Gogotsi, *Adv. Energy Mater.* **2015**, *1500589*
[27] S. T. Oyama, *The Chemistry of Transition Metal Carbides and Nitrides*, Chapman and Hall Publisher, **1996**.
[28] S. T. Oyama, *Catal. Today* **1992**, *2*, 179–200.
[29] M. Galinski, K. Babel, K. Jurewicz, *J. Power Sources* **2013**, *228*, 83–88.
[30] A. Lewandowski, P. Jakobczyk, M Galinski, *Electrochim. Acta* **2012**, *86*, 225–231.
[31] Y. Gogotsi, R. M. Penner, *ACS Nano* **2018**, *3*, 2081–2083.
[32] L. Feng, K. Wang, X. Zhang, X. Sun, C. Li, X. Ge, Y. Ma, *Adv. Funct. Mater.* **2018**, *28*, 1704463.
[33] W. Zuo, C. Xie, P. Xu, Y. Li, J. Liu, *Adv. Mater.* **2017**, *29*, 1703463.
[34] Y. Jiang, Z. Wu, L. Jiang, Z. Pan, P. Yang, W. Tian, L. Hu, *Nanoscale* **2018**, *10*, 12003–12010.
[35] Q. Jiang, N. Kurra, M. Alhabeb, Y. Gogotsi, H. N. Alshareef, *Adv. Energy Mater.* **2018**, *8* 1703043.